JAFIB
Original Research
Journal of Atrial Fibrillation

www. jafib.com

'CLOSE'-Guided Pulmonary Vein Isolation and Changes in Local Bipolar and Unipolar Atrial Electrograms: Observations from the EP Lab

Mathieu Coeman[1,2], Milad El Haddad[1,2], Michael Wolf[2], Rajin Choudhury[2], Yves Vandekerckhove[2], Sebastien Knecht[2], Rene Tavernier[2], Mattias Duytschaever[1,2]

[1]Department of Cardiology, University Hospital Ghent, Ghent, Belgium.
[2]Department of Cardiology, Sint-Jan Hospital Bruges, Bruges, Belgium.

Abstract

Background: 'CLOSE'-guided pulmonary vein isolation (PVI) is a point-by-point, contact force (CF)-guided radiofrequency (RF) approach aiming to enclose the PVs with contiguous RF lesions by targeting strict criteria for interlesion distance and ablation index (AI). We characterized real-time changes in bipolar (B-EGMs) and unipolar electrograms (U-EGMs) during AI-targeted RF delivery.

Methods: EGM changes during 56 RF applications in 7 patients with paroxysmal atrial fibrillation (AF) undergoing 'CLOSE'-guided PVI were studied. CF-guided RF was delivered with 35W targeting an AI of 400 at posterior and 550 at anterior wall. 336 B-EGMs and 336 U-EGMs before, during and after RF delivery were analyzed with their RF characteristics. Amplitude of the B-and U-EGM and morphology of the U-EGM were measured at each 5-second step using custom-made software.

Results: We observed a significant reduction in B-EGM amplitude (0.43 [IQR=0.25, 0.55] to 0.11 [0.07, 0.22] mV, p<0.001) and U-EGM amplitude (0.57 [0.40, 0.87] to 0.22 [0.10, 0.34] mV, p<0.001) within 5 seconds, after which no more changes were observed. Impedance drop was 18.3±1.1Ω. Loss of the unipolar terminal S-wave occurred in 59% of applications. There was no correlation between U-EGM morphology changes and RF characteristics.

Conclusion: In AI-guided RF delivery there is a significant reduction in EGM amplitude within 5 seconds. Loss of the unipolar terminal S wave occurred in 59% of applications and was not related to RF characteristics suggestive of adequate lesion formation. These findings suggest that there is a limited value in monitoring electrograms to further optimize 'CLOSE'-guided PVI.

Introduction

'CLOSE'-guided ablation is a point-by-point, contact force (CF)-guided radiofrequency (RF) approach aiming to enclose the pulmonary veins (PV) with contiguous and optimized RF lesions by targeting strict criteria for interlesion distance (ILD≤6mm) and ablation index (≥400 at posterior wall and ≥550 at anterior wall). This strategy is associated with a high rate of acute durable PV isolation (PVI) and favorable 1-year outcome in paroxysmal AF[1,2]. The next challenge is to further optimize 'CLOSE'-guided PVI by using site-specific ablation index target values based upon tissue characteristics before, during and after RF delivery. One of the potential candidates to assess tissue characteristics during RF application is the use of local bipolar (B-EGM) and unipolar electrograms (U-EGM) recorded by the ablation catheter. Experimental studies have shown that the occurrence of low amplitude and loss of the unipolar terminal S wave correlate with transmural lesions[3-7]. Therefore we aimed to explore the potential value of monitoring local electrogram changes during ongoing RF delivery in 'CLOSE'-guided ablation by describing the incidence, time course and characteristics of EGM changes during ablation index-targeted RF delivery.

Key Words

Catheter ablation, Atrial Fibrillation, Electrogram, Contact force.

Corresponding Author
Dr. Mattias Duytschaever, Department of Cardiology, Sint-Jan Hospital Bruges; Ruddershove 10, 8000 Bruges, Belgium

Methods

Study patients and ablation strategy

Seven consecutive patients with paroxysmal AF undergoing an AI-guided PVI at AZ Sint-Jan Hospital in Bruges, Belgium were studied. Three catheters were used for mapping and ablation: a decapolar into the coronary artery sinus, a circular decapolar catheter (Lasso, 2515 variable catheter, 2mm electrodes, 8mm spacing, Biosense Webster, Diamond Bar, CA, USA) to monitor PVI, and a 3.5 mm irrigated-tip CF ablation catheter (THERMOCOOL SMARTTOUCH®, Biosense Webster). Three-dimensional reconstruction of the left atrium (LA) was made by an electro-anatomical mapping (EAM) system (Carto, Biosense Webster). Ablation was performed at the LA-PV junction using point-by-point radiofrequency energy (mostly 35W, power controlled RF, Stockert GmbH, Freiburg, Germany). To ensure stability of the ablation catheter, Carto VisiTag module was used and preset at 8 seconds for 3mm with more than 30% ≥ 4g. Targets for ablation were an ablation index of 400 at the posterior wall and 550 at the anterior side of the circle[1,2].

In each patient, encirclement of the PVs was started with 8 distinct RF applications (4 in each circle, and 1 for each quadrant[Figure 1]).

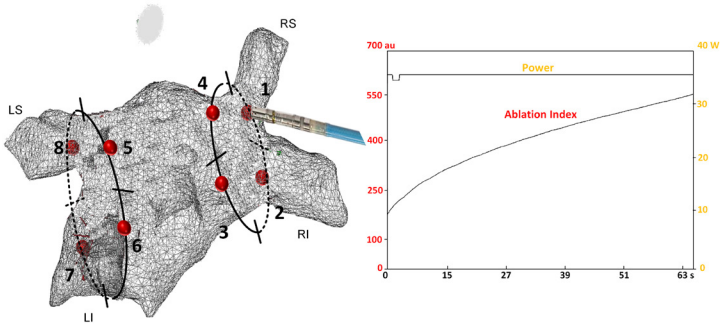

Figure 1: **In each patient, encirclement of the pulmonary veins was started with 8 distinct RF applications (4 in each circle, and 1 for each quadrant). Ablation was performed at the LA-PV junction using point-by-point RF energy (mostly 35W). Targets for ablation were an ablation index of 400 at the posterior wall and 550 at the anterior side of the circle.**

By ablating at 8 distinct sites we avoided influence from juxtaposed RF application.

EGM database

Intracardiac electrograms (unipolar, U-EGMs, and bipolar, B-EGMs) from the ablation catheter were recorded using the Carto system and sampled at 1000 Hz. B-EGMs (filtered at 30-240Hz) were recorded between the 3.5mm distal electrode and the first ring electrode. U-EGMs (filtered 0.5-500Hz) were recorded from the 3.5mm distal electrode of the ablation catheter. Using the Carto-REPLY tool (a non-commercially available tool in Carto system which allows replaying the entire procedure continuously with the possibility of capturing Carto points and EGMs retrospectively), we selected and exported for each given application, 3-second recordings before the start of the RF delivery, at 5, 10, 20 seconds during the RF delivery, at the end of RF delivery and at 5 seconds after ending the RF delivery.

EGM analysis

Using custom made software (Matlab, the MathWorks Inc, Natick, MA) we determined the amplitude and morphology of the U-EGM and B-EGM[8]. All EGMs were analyzed by an investigator (M.E.H.) blinded to the ablation protocol and RF characteristics.

Voltage of the B-EGM and U-EGM was defined as the peak-to-peak amplitude, defined as the voltage difference between the maximal positive and negative peaks. To determine the U-EGM morphology, the software determined the RS-ratio (calculated as R/(R+|S|), where R is the amplitude of the positive peak and S is the amplitude of the negative peak). An RS-ratio equal to 1 indicates a monophasic R morphology (the equivalent of loss of the terminal S deflection).

RF characteristics for a given application

For each of the 56 RF applications, we exported RF application time, average applied power, average CF, real-time circuit impedance, total impedance drop, force-time integral (FTI) and ablation index (AI). RF characteristics were compared between applications with and without a significant change in U-EGM morphology.

Statistical analysis

Statistical analyses were performed using SPSS (IBM SPSS statistics Version 24 IBM Corp, Armonk, NY, USA). Descriptive variables are presented as mean ± standard deviation when normally distributed and with median and interquartile range [1st IQR – 3rd IQR] when not normally distributed, or percentages. The student t-test or Mann-Whitney test (depending on distribution) were used for comparisons between the continuous data. Linear mixed model test accounting for multiple measures from the same patient was used to compare differences in time course. The chi-square test with a Fisher exact test was used for comparisons between the categorical data. Correlation was measured using the Pearson Correlation coefficient. A $P<0.05$ was considered statistically significant.

Study patients and ablation strategy

Seven consecutive patients with paroxysmal AF undergoing an AI-guided PVI at AZ Sint-Jan Hospital in Bruges, Belgium were studied.

Results

Database

The study patients were 65.1±8.6 years, 71.4% males with paroxysmal atrial fibrillation. Left atrial diameter was 40.0 ± 1.4mm. In total, we investigated 336 B-EGMs and 336 U-EGMs, recorded from 7 patients, at 8 different and distant ablation sites, during 6 stages of RF delivery. All patients were in sinus rhythm at the time of ablation. Applications (n=56) were characterized by a mean length of application of 24.8±2.1s at the posterior wall and 43.3±2.6s at the anterior wall. Mean CF was 13.6±0.9gr and mean impedance drop was 18.3±1.1Ohm. After the initial 8 applications, 'CLOSE'-guided encircling was continued leading to first-pass and adenosine-proof isolation in all 7 patients. The study was approved by the local institutional review committee and all patients gave informed consent.

Bipolar and unipolar EGM voltage before, during and after ablation

A representative example of ablation-induced attenuation of

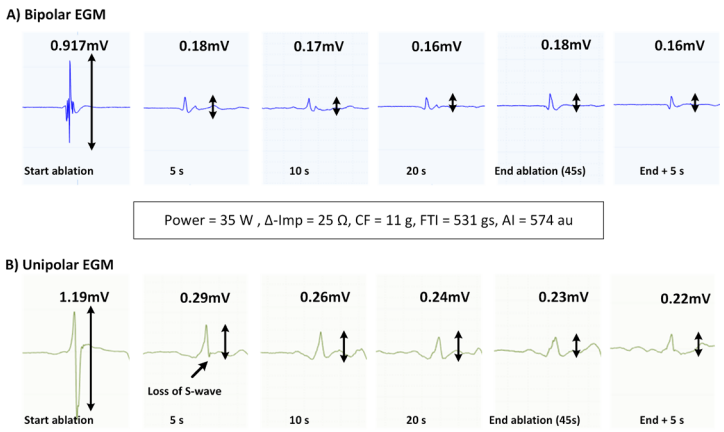

Figure 2: **Representative example of the rapid time course of ablation-induced attenuation of B-EGM and U-EGM amplitude and shift to monophasic R-wave in U-EGM during an application at the antero-inferior quadrant of the right circle (45s application reaching an ablation index of 574, impedance drop of 25Ω, CF of 11g, average power 35W).**

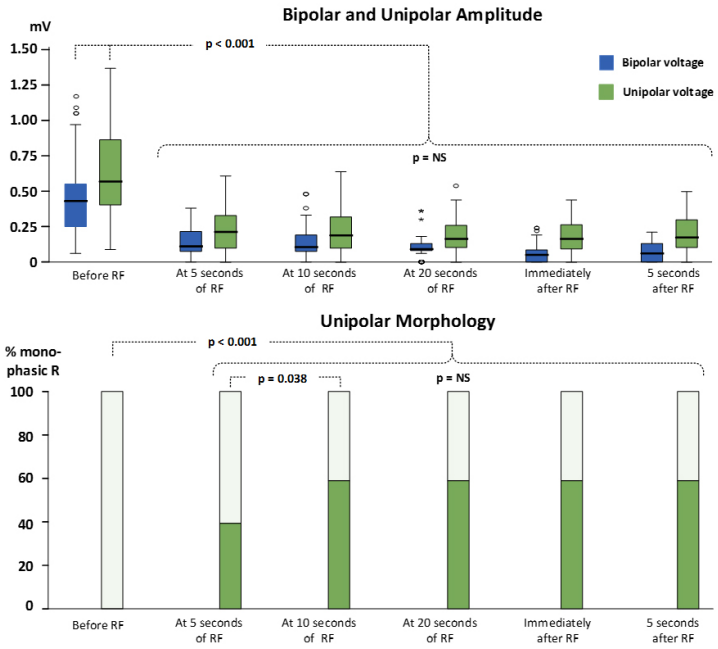

Figure 3: **Significant reduction in B-EGM and U-EGM amplitude in the first 5 seconds after which a steady state without a significant change in amplitude was seen during the rest of the duration of the ablation. The occurrence of monophasic R in U-EGM raised significantly until 10 seconds of RF application after which no more significant changes occurred.**

B-EGM amplitude is given in [Figure 2](upper panel). During this 45-sec lasting application at the antero-inferior quadrant of the right circle (until ablation index of 574, impedance drop of 25Ω, average

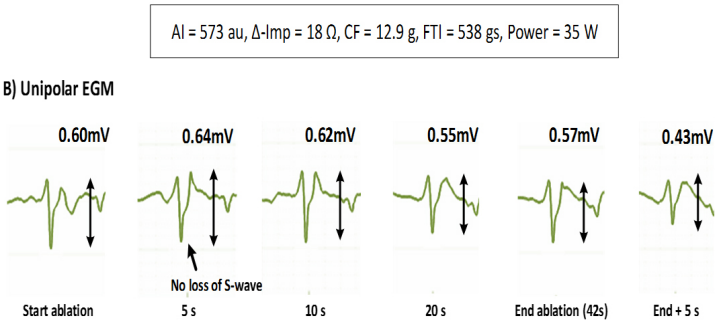

Figure 4: **During this 42-sec application (at the antero-superior quadrant of the right circle) no change occurred in the unipolar RS pattern despite delivery of 35W and reaching an ablation index of 573 and marked impedance drop (18Ω).**

CF of 11g and average power 35W), the B-EGM voltage dropped from 0.91mV to 0.18mV within 5 seconds, after which no more changes can be seen.

Overall results are given in [Figure 3]. In the first 5 seconds, there was a significant reduction in B-EGM amplitude (0.43mV [IQR = 0.25, 0.55] to 0.11mV [0.07, 0.22mV], p<0.001), after which a steady state without a significant change in amplitude was seen during the rest of the duration of the ablation.

A representative example of ablation-induced reduction in

Table 1: **Unipolar morphology change (58,9%)**

56 lesions	n=33 with change	n=23 without change	p value*
UP EGM amplitude	0.57 [0.35-0.92]	0.47 [0.31-0.71]	0.268
Power	35.0 [35.0-35.0]	35.0 [35.0-35.0]	0.19
Impedance drop	18.3 [14.2-22.6]	13.7 [11.3-23.7]	0.39
CF	11.5 [8.9-16.4]	12.2 [10.1-15.5]	0.50
FTI	479.0 [252.0-585.0]	378.0 [264.0-525.0]	0.59
AI	452.6 [437.1-567.5]	464.6 [438.0-571.9]	0.55

Comparison of ablation parameters and U-EGM amplitude before start of ablation between the group with change to unipolar monophasic R compared to applications without change to unipolar monophasic R *Mann-Whitney test

U-EGM amplitude is given in the lower tracing of [Figure 2]. Overall results are given in [Figure 3]. In the first 5 seconds there was a significant reduction in U-EGM amplitude (0.57mV [IQR = 0.40, 0.87] to 0.22mV [0.10, 0.34], p<0.001), after which a steady state without significant changes in U-EGM amplitude was observed.

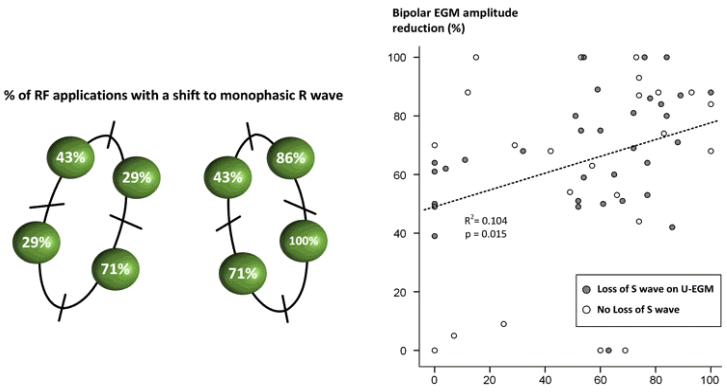

Figure 5: **Left panel: spatial distribution of the observed incidence of a shift to a monophasic unipolar R wave. Right panel: whereas B-EGM amplitude reduction and U-EGM reduction are significantly related (occurring at the same applications), the loss or no loss of S wave occurred independent of amplitude reduction**

Ablation-induced changes in the morphology of the unipolar EGM

The change in U-EGM morphology in response to ablation was inconsistent. A representative example of the loss of terminal S

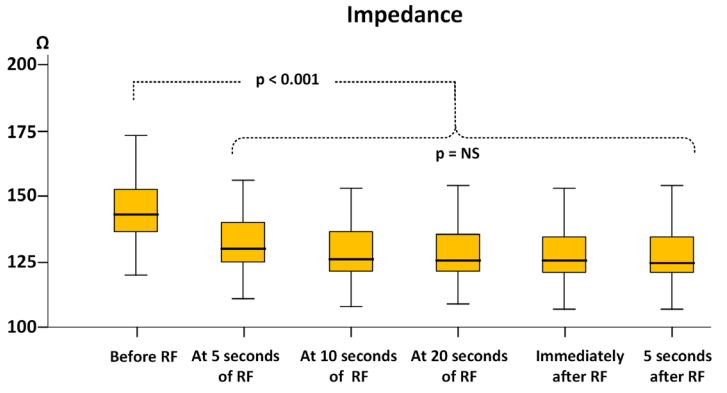

Figure 6: **Significant change of impedance in the first 5 seconds of ablation after which a steady state was observed during the rest of the duration of ablation.**

wave and its rapid time course is given in [Figure 2] (lower tracing). In [Figure 4] we plotted a representative example of a unipolar RS morphology remaining constant during a 42-sec lasting RF application (despite obtaining ablation index of 573, impedance drop of 18Ω, average CF of 12.9g and average power of 35W). Overall, the percentage of a monophasic R raised significantly from 0% before ablation to 40% after 5 seconds of ablation (p< 0.001) and from 40% after 5 seconds to 59% after 10 seconds of ablation (p=0.038) after which no more significant changes occurred [Figure 3]. Whereas overall a monophasic R was observed in 59% of application sites, patient-wise this percentage ranged from 38% to 88%, anatomy-wise from 29% (left anterior inferior site and left posterior superior site) to 86% (right anterior superior and inferior site) ([Figure 5], left panel). Comparing RF applications with and without a shift to a monophasic R, revealed no difference in delivered power (p=0.19), impedance drop (p=0.39), contact force (p=0.50), FTI (p=0.59) or ablation index (p=0.55) [Table 1]. The fact that loss or no loss of S wave occurred independent from impedance drop is nicely illustrated by comparing [Figure 2](loss of S wave and impedance drop 25 Ω) and [Figure 4] (no loss of S wave despite impedance drop of 18 Ω). Applications without a shift to monophasic R had also a comparable U-EGM amplitude at baseline. Finally, loss or no loss of the terminal S wave occurred independent of the reduction in U-or B-EGM amplitude ([Figure 5], right panel).

Ablation-induced impedance changes

The overall mean impedance drop was 18.3±1.1Ω or 9.4±6.1%. Similar to the time course of the U-and B-EGM amplitude and loss of S wave, we observed a rapid impedance decrement [Figure 6]. Mean baseline impedance was 144±11.6Ω and fell to 131±10.6Ω (p<0.001) within 5 seconds. Between 5 and 10 seconds there was a further but non-significant decrease to 128±10.6Ω (p=0.09) after which a steady state without a significant change in impedance was seen during the rest of the duration of the ablation.

Discussion

Major findings

During stable CF- and AI-guided RF delivery we observed a significant reduction in bipolar and unipolar electrogram amplitude within the first 5 seconds after ablation. Loss of the unipolar terminal S wave was an inconsistent finding and not related to RF characteristics suggestive of adequate lesion formation. These findings suggest that in the current clinical setting - characterized by far field recording and micro-shifting of the catheter - there is limited value of monitoring real-time changes in local electrograms in the clinical quest to further optimize 'CLOSE'-guided PVI.

The clinical setting of the above findings is both the strength and weakness of the present study. Whereas lack of animal data precludes histological lesion assessment, the obtained data are clinically relevant because directly obtained from the cathlab and obtained with a technique invariably leading to marked impedance drop and clinical durable PVI in patients.

Voltage attenuation as a marker for lesion depth

In vivo experimental data have shown that transmural lesions (as assessed by histology) were associated with an average 41% reduction in B-EGM (porcine atria) and that EGM amplitude was decreased significantly more at transmural vs non-transmural sites (by 63% vs 42% in B-EGMs and by 49% vs 15% in U-EGMs) (bovine atria) [6-7]. Furthermore, there is a widespread clinical use of electrogram attenuation (especially in B-EGM) as a criterion to titrate RF delivery, with ablation strategies using a 50 to 90% diminution threshold as a surrogate for adequate lesion formation[9-15].

In the present study we confirmed a significant ablation-induced reduction in bipolar and unipolar voltage during stable, AI-guided RF energy. Together with the marked impedance drop, those data are consistent with adequate lesion formation using the current ablation strategy.

The rapid onset of voltage attenuation however seems to limit its clinical utility for monitoring lesion formation. In fact, in the present clinical approach, RF delivery was continued for another 15 (posterior wall) to 35 seconds (anterior wall) after the onset of voltage attenuation in order to reach the required ablation index. This time course is in line with experimental data. In vitro and in vivo studies have shown that the half-time of lesion growth is approximately 7 to 10 seconds, and maximum lesion size is achieved after 30 to 40 seconds of RF delivery[16-18]. Likewise, Gepstein et al showed that RF applications lasting 10 seconds longer than 80% U-EGM amplitude reduction were associated with lesion continuity (conduction block and histology in 8 right porcine atria) after 4 weeks[3]. Finally, this observation is in line with a recent study in 11 sheep in which RF ablation was performed using direct lesion visualization. Despite the occurrence of a significant (>50%) voltage drop in U-EGM occurring in 94% of lesions at a mean duration of 7 seconds, lesion volume (surface area) continued to grow in the first 23±5.8 seconds[19].

Of interest, the time course of electrogram attenuation paralleled the time course of impedance drop [Figure 6]. Also this observation is in line with the study of Bhaskaran et al. in which a significant decrement (20%) in circuit impedance occurred in 94% of the ablations at 8.5±7.2 seconds (which was 13.1±7.9 seconds earlier than the observed endocardial lesion maturation)[19].

Loss of the terminal S wave in unipolar electrograms

Elimination of the terminal negative deflection in the unipolar electrogram (loss of the terminal S wave) is associated with lesion transmurality and thus useful to assess lesion depth and monitor lesion formation. This concept, based upon the morphology of the unipolar electrogram was introduced and validated by the experimental work of Otomo et al in the in-vivo swine model[4,20]. Using a model of fixed 30-s RF applications in smooth atrial tissue, investigators obtained applications with and without transmurality at histology. On EGM analysis, transmural lesions (n=54) invariably exhibited elimination of the negative deflection (irrespective of catheter orientation), whereas those from non-transmural lesions (n=71) did not[4]. Likewise Bortone et al showed in a closed-dog model that elimination of the negative component of the unipolar atrial electrogram reflects, in general, irreversible transmural necrosis creation[5]. Of interest, the same research group described recently a CF-guided ablation strategy in which RF is continued 5 to 15s after elimination of the negative component which apparently was obtained in all applications [21].

In the present clinical study we observed a loss of the unipolar

terminal S wave in only 59% of applications. Several mechanisms may account for this relatively low incidence. (1) First, one might hypothesize that the lack of changes in U-EGM morphology indicates that AI-guided RF delivery does not invariably lead to transmural lesions. Although the current ablation strategy is associated with marked Δ-Imp and high acute and 1-year durable PV isolation and although there was no difference in RF characteristics (including Δ-imp) between lesions with or without loss of the S wave, we cannot refute this hypothesis without evidence of histology. (2) Second, low incidence might be explained by the strict algorithmic definition used in the present study. Vice versa, it is plausible that the incidence of a loss of S wave is overestimated when evaluated visually. Not surprisingly, in another clinical study in 18 patients, elimination of the terminal S wave in unipolar electrograms was observed in only 64% of applications (and at a median of 2.3 seconds) and no correlation with dormant conduction could be made [22]. (3) Third, discrepancy in results might be explained by differences in recording and ablation settings. It is known that different filter settings can affect the morphology of the unipolar electrogram. Also the use of large tip electrodes might result in farfield sensing. More recently, Kumar et al showed that the actual incidence of voltage attenuation or loss of unipolar R wave was clearly dependent on the irrigation rate (with a very low incidence in high flow ablation like in the present study)[23]. (4) Finally, in the clinical setting - in contrast to experimental models - variables like catheter orientation, micro-shifting of the ablation catheter tip, complex architecture (ridges, crypts and valleys), tissue thickness and composition come into play.

It seems, that as long as we cannot overcome these limitations in the clinical setting, there is a limited potential of monitoring unipolar electrograms to optimize 'CLOSE'-guided PVI. In fact, in the current ablation protocol, ablation until loss of the terminal S wave would have resulted in applications of 5 to 10 sec in 60% of the applications [Figure 2] whereas in other applications [Figure 4] absence of change would have led to unnecessary continuation of RF delivery.

Future research

Further optimization of catheters, filtering and recording might improve clinical utility of local electrograms in guiding ablation. It remains to be seen whether micro-electrodes on the tip of the catheter are useful to assess lesion depth and monitor lesion growth. In a small canine study, transmurality could be reliable achieved by titration of RF until stop of attenuation of a micro-electrode bipolar EGM amplitude, in contrast with the tip-ring bipolar EGM which was highly unreliable[24]. In another study in 13 canines by the same group, mean EGM attenuation recorded from the tip-ring bipolar EGM was 44% whereas the mean reduction from the micro-electrode bipolar EGM was 82% [25]. Of interest, in this study a rapid decrease in EGM amplitude was followed by a more gradual reduction which reached a plateau after 8 seconds in thin atrial tissues.

Limitations

This was a small, single-center, clinical study. The correlation between EGM parameters and AF recurrence after ablation was not investigated. No data are available on catheter orientation during recording and ablation. No histological data were available.

Conclusion

In AI-guided RF delivery there is a significant reduction in EGM amplitude within 5 seconds. Despite a consistent and marked impedance drop, loss of the unipolar terminal S wave occurred in only 59% of applications. These findings may suggest that there is a limited value in monitoring electrograms to further optimize 'CLOSE'-guided PVI.

References

1. P Taghji, M El Haddad, T Phlips, M Wolf, S Knecht, Y Vandekerckhove, R Tavernier, H Nakagawa, M Duytschaever. Evaluation of a Strategy Aiming to Enclose the Pulmonary Veins With Contiguous and Optimized Radiofrequency Lesions in Paroxysmal Atrial Fibrillation: A Pilot Study. JACC: Clinical Electrophysiology. 2017;6:23.
2. El HM, Taghji P, Phlips T, Wolf M, Demolder A, Choudhury R, Knecht S, Vandekerckhove Y, Tavernier R, Nakagawa H, Duytschaever M. Determinants of Acute and Late Pulmonary Vein Reconnection in Contact Force-Guided Pulmonary Vein Isolation: Identifying the Weakest Link in the Ablation Chain. Circ Arrhythm Electrophysiol. 2017;10 (4).
3. Gepstein L, Hayam G, Shpun S, Cohen D, Ben-Haim S A. Atrial linear ablations in pigs. Chronic effects on atrial electrophysiology and pathology. Circulation. 1999;100 (4):419–26.
4. Otomo K, Uno K, Fujiwara H, Isobe M, Iesaka Y. Local unipolar and bipolar electrogram criteria for evaluating the transmurality of atrial ablation lesions at different catheter orientations relative to the endocardial surface. Heart Rhythm. 2010;7 (9):1291–300.
5. Bortone A, Brault-Noble G, Appetiti A, Marijon E. Elimination of the negative component of the unipolar atrial electrogram as an in vivo marker of transmural lesion creation: acute study in canines. Circ Arrhythm Electrophysiol. 2015;8 (4):905–11.
6. Sanchez Javier E, Kay G Neal, Benser Michael E, Hall Jeffrey A, Walcott Gregory P, Smith William M, Ideker Raymond E. Identification of transmural necrosis along a linear catheter ablation lesion during atrial fibrillation and sinus rhythm. J Interv Card Electrophysiol. 2003;8 (1):9–17.
7. Koa-Wing M, Kojodjojo P, Malcolme-Lawes LC, Salukhe TV, Linton NW F, Grogan AP, Bergman D, Lim PB, Whinnett ZI, McCarthy K, Ho SY, O'Neill MD, Peters NS, Davies DW, Kanagaratnam P. Robotically assisted ablation produces more rapid and greater signal attenuation than manual ablation. J. Cardiovasc. Electrophysiol. 2009;20 (12):1398–404.
8. El HM, Houben R, Berte B, Van HF, Stroobandt R, Vandekerckhove Y, Tavernier R, Duytschaever M. Bipolar electrograms characteristics at the left atrial-pulmonary vein junction: Toward a new algorithm for automated verification of pulmonary vein isolation. Heart Rhythm. 2015;12 (1):21–31.
9. Vest John A, Seiler J, Stevenson WG. Clinical use of cooled radiofrequency ablation. J. Cardiovasc. Electrophysiol. 2008;19 (7):769–73.
10. Oral H, Scharf C, Chugh A, Hall B, Cheung P, Good E, Veerareddy S, Pelosi F, Morady F. Catheter ablation for paroxysmal atrial fibrillation: segmental pulmonary vein ostial ablation versus left atrial ablation. Circulation. 2003;108 (19):2355–60.
11. Pokushalov E, Romanov A, Corbucci G, Artyomenko S, Turov A, Shirokova N, Karaskov A. Ablation of paroxysmal and persistent atrial fibrillation: 1-year follow-up through continuous subcutaneous monitoring. J. Cardiovasc. Electrophysiol. 2011;22 (4):369–75.
12. Ullah W, McLean A, Tayebjee MH, Gupta D, Ginks MR, Haywood GA, O'Neill M, Lambiase PD, Earley MJ, Schilling RJ. Randomized trial comparing pulmonary vein isolation using the SmartTouch catheter with or without real-time contact force data. Heart Rhythm. 2016;13 (9):1761–7.

13. Stabile G, Bertaglia E, Senatore G, De SA, Zoppo F, Donnici G, Turco P, Pascotto P, Fazzari M, Vitale DF. Catheter ablation treatment in patients with drug-refractory atrial fibrillation: a prospective, multi-centre, randomized, controlled study (Catheter Ablation For The Cure Of Atrial Fibrillation Study). Eur. Heart J. 2006;27 (2):216–21.
14. Pappone C, Rosanio S, Oreto G, Tocchi M, Gugliotta F, Vicedomini G, Salvati A, Dicandia C, Mazzone P, Santinelli V, Gulletta S, Chierchia S. Circumferential radiofrequency ablation of pulmonary vein ostia: A new anatomic approach for curing atrial fibrillation. Circulation. 2000;102 (21):2619–28.
15. ME J. Josephson's Clinical Cardiac Electrophysiology. 5th ed. Philadelphia: Wolters Kluwer/Lippincott Williams and Wilkins. 0;126:63–73.
16. DE H. Determinants of Lesion Size During Radiofrequency Catheter Ablation: The Role of Electrode-Tissue Contact Pressure and Duration of Energy Delivery. Journal of Cardiovascular Electrophysiology . 1991;126:63–73.
17. Simmers T A, Wittkampf F H, Hauer R N, Robles de MedinaE O. In vivo ventricular lesion growth in radiofrequency catheter ablation. Pacing Clin Electrophysiol. 1994;17 (3 Pt 2):523–31.
18. Wittkampf F H, Hauer R N, Robles de Medina E O. Control of radiofrequency lesion size by power regulation. Circulation. 1989;80 (4):962–8.
19. Bhaskaran A, Chik W, Nalliah C, Pouliopoulos J, Barry T, Nguyen DT, Midekin C, Samanta R, Farraha M, Thomas S, Kovoor P, Thiagalingam A. Observations on Attenuation of Local Electrogram Amplitude and Circuit Impedance During Atrial Radiofrequency Ablation: An In vivo Investigation Using a Novel Direct Endocardial Visualization Catheter. J. Cardiovasc. Electrophysiol. 2015.
20. Spach M S, Miller W T, Geselowitz D B, Barr R C, Kootsey J M, Johnson E A. The discontinuous nature of propagation in normal canine cardiac muscle. Evidence for recurrent discontinuities of intracellular resistance that affect the membrane currents. Circ. Res. 1981;48 (1):39–54.
21. Bortone A, Lagrange P, Cauchemez B, Durand C, Dieuzaide P, Prévot S, Mechulan A, Pambrun T, Martin R, Parlier P, Masse A, Marijon E, Albenque JP. Elimination of the negative component of the unipolar electrogram as a local procedural endpoint during paroxysmal atrial fibrillation catheter ablation using contact-force sensing: the UNIFORCE study. J Interv Card Electrophysiol. 2017;49 (3):299–306.
22. Iso K, Okumura Y, Watanabe I, Nagashima K, Sonoda K, Kogawa R, Sasaki N, Takahashi K, Kurokawa S, Nakai T, Ohkubo K, Hirayama A. Wall thickness of the pulmonary vein-left atrial junction rather than electrical information as the major determinant of dormant conduction after contact force-guided pulmonary vein isolation. J Interv Card Electrophysiol. 2016;46 (3):325–33.
23. Kumar S, Romero J, Stevenson WG, Foley L, Caulfield R, Fujii A, Tanigawa S, Epstein LM, Koplan BA, Tedrow UB, John RM, Michaud GF. Impact of Lowering Irrigation Flow Rate on Atrial Lesion Formation in Thin Atrial Tissue. JACC: Clinical Electrophysiology . 2017;3:1114–1125.
24. HP Avitall B, D Vance, J. Koblish. Determinants of atrial lesion maturation during radio frequency ablation using localized tissue electrograms. . J Innov Cardiac Rhythm Manage . 2014;5:1574–1585.
25. Avitall B, Horbal P, Vance D, Koblish J, Kalinski A. Maximal electrogram attenuation recorded from mini electrodes embedded on 4.5-mm irrigated and 8-mm nonirrigated catheters signifies lesion maturation. J. Cardiovasc. Electrophysiol. 2015;26 (2):192–202.